International Conference on Mathematics, Computational Methods & Reactor Physics (M&C 2009)
Saratoga Springs, New York, May 3-7, 2009, on CD-ROM, American Nuclear Society, LaGrange Park, IL (2009)

TESTING OF THE TETRAHEDRAL MESH IMPORT CAPABILITY FOR IMPORTING CONVERTED CAD FILES FOR SHIELDING AND CRITICALITY CALCULATIONS WITH MONK AND MCBEND

Adam Bird, Julie Martin, Edmund Shuttleworth
Serco
Winfrith, Dorchester, Dorset, DT2 8DH, UK
Adam.Bird@ sercoassurance.com; Julie.Martin@sercoassurance.com

Andrew Cooper
Sellafield Ltd
Andrew.J.Cooper@sellafieldsites.com

ABSTRACT

The ANSWERS software service has developed a tetrahedral mesh import capability for the shielding and criticality Monte Carlo codes MONK and MCBEND. The purpose is to provide a means to import CAD geometries that have been converted to a tetrahedral mesh using a meshing program. The speed of the calculation is not dependent on the mesh size and is only 5 to 50% slower than the equivalent model using the solid body geometry package of MONK and MCBEND. This paper investigates the accuracy of the method which using realistically complex models has shown a 5 – 10% variation in the results of MCBEND calculations from an equivalent solid body geometry model. The investigation concludes that the differences can be attributed to the approximation of primitive bodies by tetrahedra.

Key Words: CAD Import Monte Carlo

1. INTRODUCTION

Reactor components (e.g. fuel assemblies) and other equipment (e.g. transport flasks) are designed using Computer Aided Design (CAD) packages. It is useful to be able to directly use these geometries in Monte Carlo calculations. The root of the problem is as follows. MCBEND [1] and MONK [2], in common with other Monte Carlo programs, use Constructive Solid Geometry (CSG) a geometry system based on simple geometric bodies, for example cuboids, cylinders, ellipses and tori, whereas CAD programs generally use Boundary Representation (B-rep) consisting of higher-order shapes, typically represented as Non Uniform Rational B-Spline (NURBS) surfaces. There is no general method of accurately converting a B-rep model into a CSG model.

There are two broad approaches to this problem. One is to use the CAD package itself to perform the particle tracking and form a link between the Monte Carlo code and the CAD package. This can tie the system to a particular CAD package and be detrimental to the performance of the Monte Carlo calculation. A second method is to implement NURBS geometry tracking routines in the Monte Carlo program. This is a non-trivial exercise and is the subject of current work under the Nuclear Code Development partnership (NCD) between Serco and Sellafield Ltd [3].

The alternative of a tetrahedral mesh import capability was the result of looking for a simplified approach to the problem of tracking through CAD geometries in Monte Carlo codes. This paper reports some of the testing of this capability; including a realistically complicated geometry.

2. DESCRIPTION OF THE METHOD

The approach chosen is to convert the CAD model into a format that is easier to track in Monte Carlo codes. The format chosen is a tetrahedral mesh representation. There is a considerable amount of software available on the market for converting CAD models into meshes of tetrahedra. Serco has used the ICEM-CFD workbench to produce meshes. ICEM-CFD is part of the CFX modelling package, which has powerful meshing capabilities including functions for cleaning 'dirty' or 'bad' CAD. Once the mesh is read into MONK/MCBEND it is treated as a Hole geometry that uses Woodcock tracking. The software structure of MONK/MCBEND make it easy to include a Hole geometry as a self contained geometry type that can be freely used with all the existing geometry options.

2.1. Woodcock tracking as used by the Hole geometry package of MONK/MCBEND

MONK and MCBEND share the same geometry modelling capabilities. This geometry function consists of two parts; a simple body component known as Fractal Geometry, and a component implementing Woodcock tracking known as Hole Geometries.

Fractal Geometry (FG) is a system of solid geometry modelling for Monte Carlo particle tracking codes. The principal objective is to subdivide the problem space into volumes (*zones*) of uniform material. Individual zones are defined as unions, intersections and differences of simple mathematical *bodies* such as cuboids, cylinders and spheres. The problem to be specified may be divided into a hierarchical system of *parts* to simplify the construction and to take advantage of any replication which may be present.

Particle tracking techniques based on the simple solid body geometry system that rely on finding the intersection of a particle track with a body surface have potential limitations: only bodies defined by equations that can be efficiently solved can be employed. Attempting to model some replicating and complex components in a realistic manner can result in inefficiencies due to the large number of bodies and surfaces involved.

Finding the intersection of a particle track with a body surface is necessary only because the mean free path varies between materials. If the mean free path could be made constant within a volume of space, then the process of tracking to surfaces could be replaced by the rather easier task of determining the material present at a collision point. Since the mean free path is not naturally constant between materials, artificial extra cross-sections can be introduced into materials so that the total cross-section, and hence the mean free path, is constant for all materials in a particular volume of space. To maintain the correctness of the model collisions that occur because of the additional cross-sections are ignored, these are known as pseudo

collisions. This is the principle of Woodcock tracking. No approximations are involved in Woodcock tracking.

2.2. The tracking process in the mesh Hole

Once the mesh model has been read, the requirements of MONK and MCBEND are to be able to query the mesh and find the material that is present at a point **p**. This is a matter of finding which tetrahedral contains point **p**. The search process simply scans a list of candidate tetrahedra until one is found that fits the criterion.

One aspect of the Woodcock tracking system employed in Hole geometries is that no assumption can be made about where the track has come from, because we are only ever interested in where we are now, so it is not easy to simply search the neighbours of the last tetrahedral that was encountered. In fact, when this method was implemented it was found to slow the calculation. It was found that the fastest method was to divide the volume containing the mesh into voxels, which are equal-sized cubes aligned with the model axis. First the voxel containing point **p** is determined, then the tetrahedra that overlap that voxel are tested to determine which tetrahedron and hence which material is at point **p**. [4] describes other optimizations that are applied.

2.3. The problem of mapping tetrahedra to material compositions

Any CAD import system for Monte Carlo has to determine how to reconcile a position in the model with the correct material composition. The ANSYS meshing package will assign a name to groups of tetrahedra; this name might be associated with the original entity in the CAD model or created by the user during the meshing process. In MCBEND and MONK these names in the mesh file become ‘alpha-numeric’ named materials in the MONK or MCBEND input file and are simply referenced to material compositions defined in the input by the modeller.

2.4. Dealing with undefined volumes within the mesh

Undefined volumes in mesh files can occur for several reasons. Typically CAD models only define the solid real material components of a model leaving voids undefined. When the model is meshed these remain undefined. In addition errors can occur in the meshing process that can leave undefined sliver volumes between the surfaces of what should have been co-incident boundaries in the CAD model. An undefined volume can cause problems for a Monte Carlo program.

A Hole in MONK and MCBEND is always infinite in extent and is cut back by the boundaries of the FG zone it is placed in. For Holes that represent geometries that are not infinite an exterior or interstitial material is assigned. Thus for the Mesh Hole anywhere that is not defined by a tetrahedra becomes the interstitial material, with the default being void. This means that volumes of space that were voids in the original CAD model become VOIDS in the MCBEND or MONK model. Treating a sliver volume as a void is not likely to significantly impact a

calculation since they are very small volumes. It is possible to visualize these so the modeller can make an assessment of the likely impact.

2.4. Multiple mesh files

MCBEND and MONK are able to load multiple mesh files into a single calculation. These could be sourced from different CAD models or from parts of the same CAD model if components of the model have been meshed separately to make the meshing more efficient. Each mesh file becomes a mesh Hole. Each mesh Hole can be used any number of times within the geometry. A mesh Hole can be used as the interstitial material of another mesh Hole.

2.5. Volumes of materials within the Tetrahedral mesh

For the purposes of this testing a development was made to the tetrahedral mesh Hole to sum the volumes of all the tetrahedra associated with each alpha-numeric named material which is processed from the original CAD model as noted in section 2.3. Material volumes can also be calculated analytically for some simple body configurations or can be calculated stochastically by MCBEND. The comparison of material volumes is discussed later.

3. TEST CALCULATIONS

This section describes two of the test models that have been used. These are:

- A Transport flask. A realistic model with exact FG equivalent.
- A Box and Pipe. A simple model with exact FG equivalent.

The transport flask is a realistic model that was used for testing much of the initial development of this capability and for the speed trials reported in [4]. The flask Mesh calculation consistently underestimated the flask FG calculation which prompted this investigation of accuracy. Several very simple models were created to test the accuracy of the Mesh Hole, the box and pipe case is the example that is reported here.

3.1. Box and Pipe

This is a simple example consisting of a ‘U’ shaped tube joined to a box. The box and the tube are hollow with walls 2cm thick. This simple model with the ‘U’ shaped tube was chosen because a tetrahedral mesh cannot exactly model the curved surface and as such would provide a good test of the extent to which meshing inaccuracies would affect the calculation.

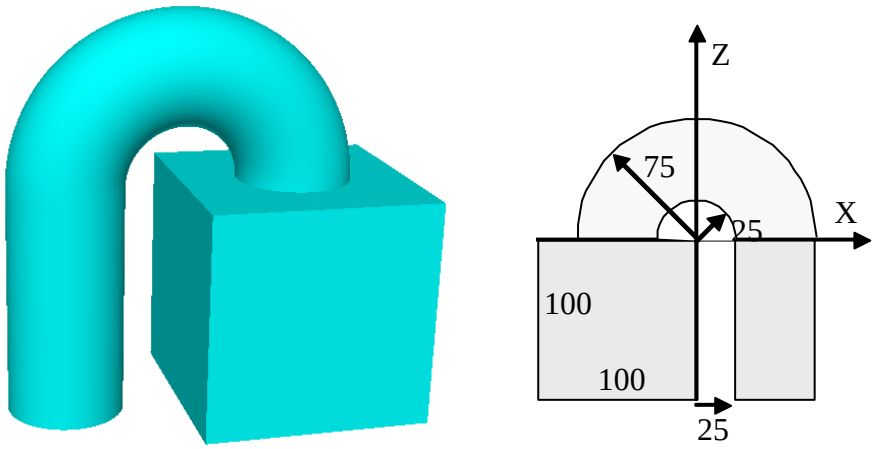

Figure 1. Box and Pipe model.

The mesh model comprised 123,000 tetrahedra. Material 1 (the body walls) and material 2 (otherwise material) were defined to contain the fictitious nuclide Cr[1]. A density of 1.0 is assigned to the material of the box and pipe and a density of 0.01 is used everywhere else. A uniform source of intensity 0.02 (particles/second/cc) covers the entire model.

3.1.1 Calculation of Material volumes

The material volumes in the Mesh model and the FG model can be calculated analytically and stochastically by the tally module.

Table I comparisons of material volumes between the Mesh and FG cases

	Mesh	**FG**
V analytical	96,835	96,572
V sampled	96,628	96,408
σ	±0.68%	±0.68%
Δ (σ units)	-0.314	-0.25

The sampling estimate used 1,000,000 points. All the estimates were lower than the analytical values but the agreement is within acceptable statistical error.

It is slightly curious that the Mesh volumes (analytical and sampled) are slightly greater than the FG model volumes. The Mesh of a curved surface is circumscribed by the true curve and it is therefore expected that the Mesh volumes should be less than the FG model.

[1] ASWERS uses a set of fictitious nuclides with simple properties that facilitate analytical solutions to some problems and provide a means of testing MONK and MCBEND independently of the nuclear data [5].

Consider the simple model in figure 2 in which an annulus is triangulated.

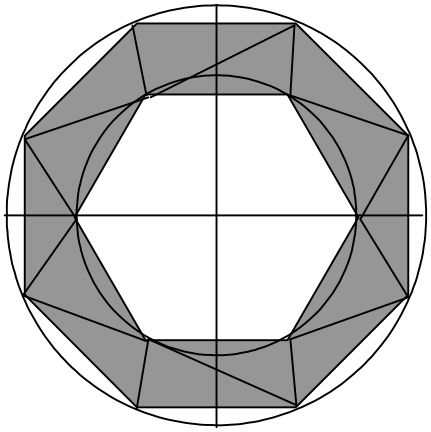

Figure 2. Triangulation of a simple annulus.

In this simple sketch the outer circle of the annulus is approximated by an octagon; the inner by a hexagon. If the inner and outer radii are 0.98 and 1.0 respectively the true annular area is 0.1244; the triangulated approximation is 0.333. This could be an explanation for the pattern of volumes (Mesh > FG) observed above. The details of the tetrahedral representation of the pipe and torus are not known but if the inner surfaces of the walls have fewer nodes than the outer surfaces then this behaviour could occur.

3.1.2. Test Calculations

A scoring mesh was used as shown in the Figure 3

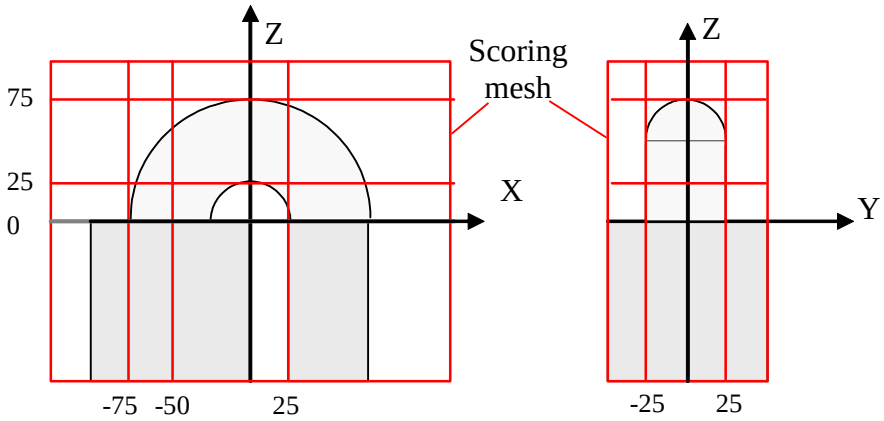

Figure 3. Location of overlaid scoring mesh.

Scoring by material was requested so that the scoring module calculates the volume of material in each mesh. The scoring meshes were examined to determine if any scores had occurred in a

material that was not supposed to be in that mesh. For the FG case none were found, as would be expected. For the Mesh case some spurious results were found, the distribution of these indicated that the box extends slightly above the Z=0 plane. The spurious volume corresponds to an intrusive Z thickness of about 0.072 ± 0.016cm. When we consider that the minimum Z vertex coordinate was -99.934 which is 0.066cm above the expected limit of -100cm it suggests that the box, at least, in the mesh model was not positioned exactly as expected.

If you consider the top half of figure 2 as the curved pipe then you can see that the maximum Z position of the mesh model is below that of the FG model. Closer inspection of the mesh file revealed that this is the cause of the offset.

Despite the differences between the FG and Mesh models the flux calculations agreed well, although the uncertainties were between 1 and 2% so any small discrepancies would have been lost.

A further test was carried out modifying the mesh case by masking with the FG model after offsetting 0.066 cm higher to match the mesh. In this calculation there should be no materials from the mesh sampled. Using 10,000,000 sample points the scoring module recorded a total of 1 sample points hitting material 1 from the mesh model. One spurious point in 10 million samples seems to be an acceptable result.

The FG model mask was modified to remove the interior of the straight and curved sections of the pipe. This should allow a small volume of material 1 to become visible because the inner boundaries of the pipes are polyhedra that inscribe the inner pipe radii.

The volume scores are:

lower subdivision (cylindrical pipe): `850.5 ±2.30%`
lower subdivision (curved pipe): `1571.4 ±1.69%`

These volumes are about 5% of the true volumes of the pipe walls for both bodies.

3.1.3. Summary

These conclusions strictly apply only to the model analysed here but could have more general relevance.

If an FG model is a correct equivalent of a Mesh representation there are no significant differences that cannot be attributed to the approximation of primitive bodies by tetrahedra.

A CAD model processed into a Mesh hole may not be exactly the same as the geometry model originally specified.

3.2. Transport Flask

This is a stainless steel and lead flask typically used for transporting gamma-ray sources. A Visual Workshop [6] generated image of the FG model is shown in Figure 4. The flask is about 1.2 meters high, 34cm radius with fins extending a further 8.95 cm.

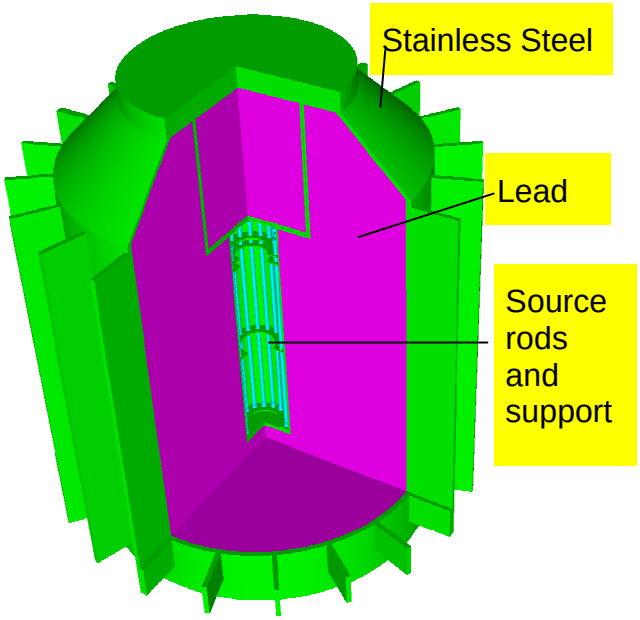

Figure 4. FG model of the transport flask.

Two mesh models of the whole flask including detail of the source rods were used for this testing. Mesh 1 comprising 120,957 tetrahedra and mesh 2 comprising 919,386 tetrahedra. Figure 5 shows the difference in the detail of the source rods and support structure for the two meshes.

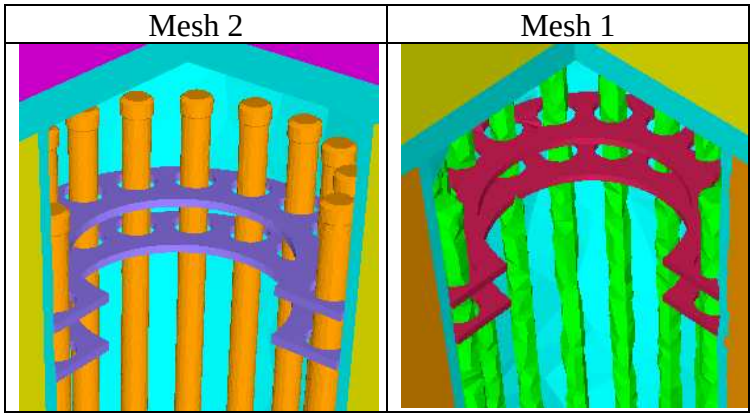

Figure 5. Comparison of the 2 mesh models.

3.2.1. Problems encountered from the test calculations

Energy deposition was scored at locations in an overlaid scoring mesh through the flask and gamma-ray dose was scored axially outside the flask. These scoring locations are displayed in Figure 6.

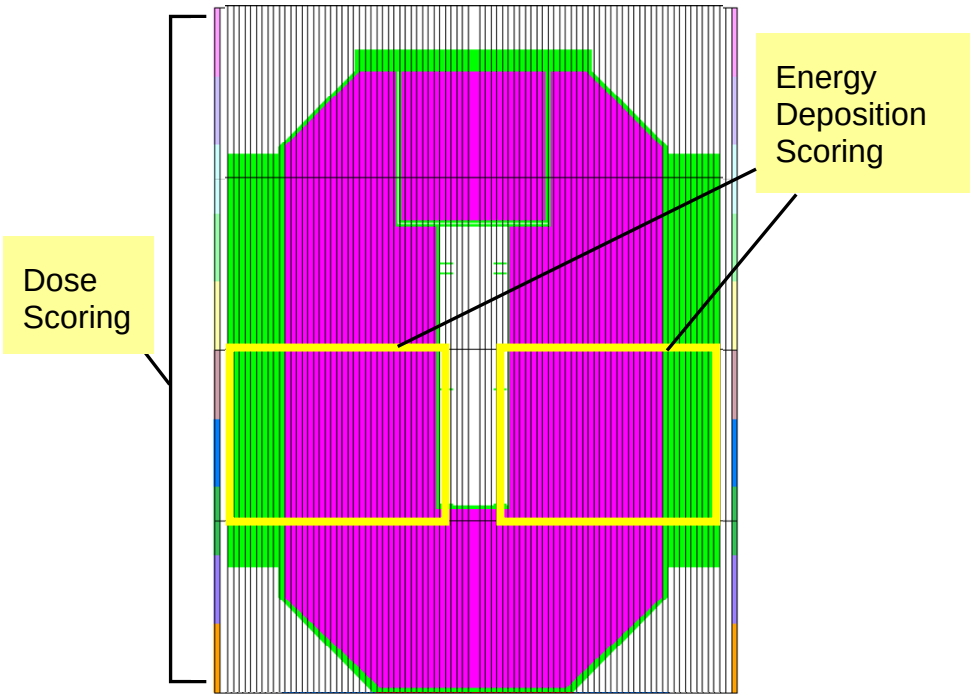

Figure 6. Location of the scoring regions in the flask model.

As reported in [3] the speed of the calculation is not dependent on the number of tetrahedra. The standard deviation on the gamma dose results are between 0.5% and 2%. The Mesh models ran about 30% slower than the FG case. Figure 7 shows the ratio of the FG result to the Mesh model results. There are two points of concern here:

- An approximate 5% underestimate in the Mesh results compared to the FG model.
- The large (ratio of 0.75) under estimate in the uppermost scoring region (10).

Hole geometries give the same result as the equivalent Solid body model so it is likely that the discrepancy is caused by approximations introduced in the meshing process.

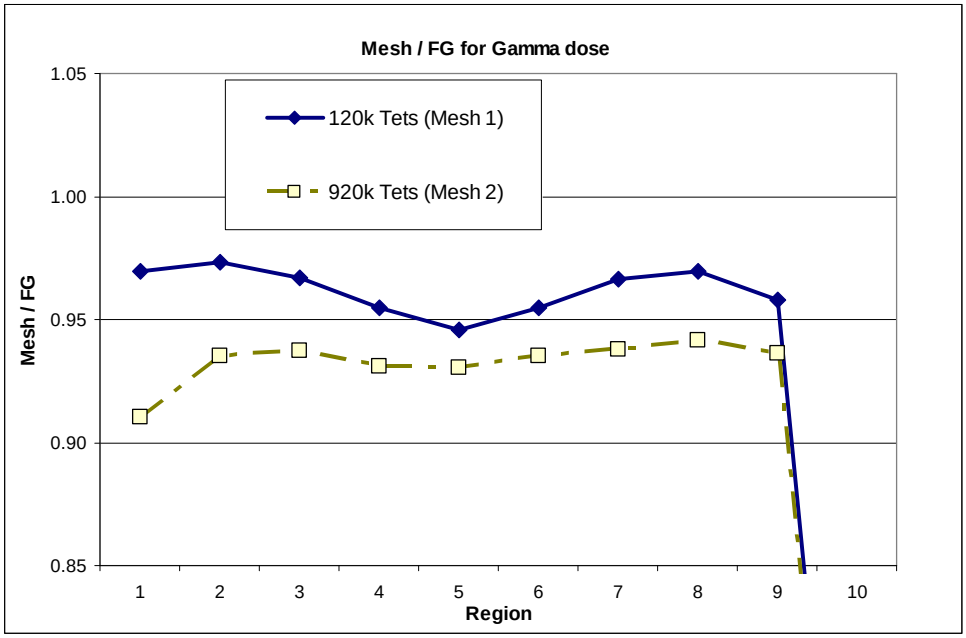

Figure 7. Ratio of FG result to the Mesh model result.

A large under estimate in the result is seen for scoring region number 10. This scoring region is near the top of the flask and as such we would expect a contribution from a streaming path around the lid of the flask. The streaming path is a 1 mm cylindrical shell of void. Features of this sort are not meshed very well and in both mesh models the void is 'patchy' rather than continuous.

The agreement of the energy deposition results between the mesh and FG models is shown in Figure 8. Most of the standard deviations on the results are less than 1%. Other points to note are:

- A large fluctuating variation in the inner radial intervals which include the source basket.
- A ratio of 0.92 – 0.9 up to about mesh 23.
- Some fluctuation about the 0.9 ratio in radial meshes 24 – 29. These fluctuations correspond to results with higher standard deviations (1 – 4%) on the 'edges' of two calculations. The first calculation used an importance function targeting the outside of the flask so the spectrum will be progressively less suitable for scoring energy deposition as you move towards the centre of the flask. The second calculation was analogue (no importance function) with increasing variance with increasing radius.
- From about the 29th radial division the result settles down to a ratio between 0.93 – 0.94.
- There is a large underestimate in the last radial mesh. This includes the fins and could be due to differences in the modelling of the ends of the fins.

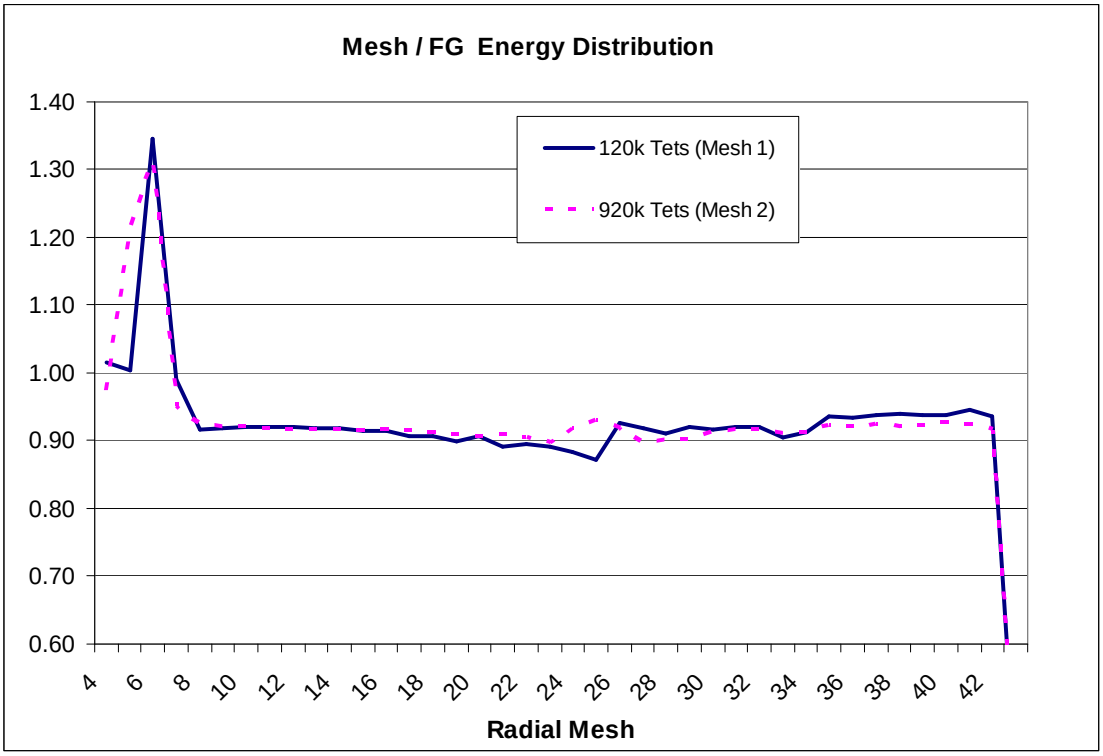

Figure 8. Ratio of FG result to the Mesh model result.

3.2.2. Analysis

The source in this case is Co^{60} which emits two gamma rays with energy 1.33 and 1.17MeV. A factor of 0.95 corresponds to an extra attenuation through 0.051 mean-free-paths (mfp) of material. Table II converts this to thicknesses **t** for the component materials of the case.

Table II mean-free-path and the corresponding additional thickness 't' required to reduce the result by a factor of 0.95

Material	**Stainless**	**Cobalt**	**Lead**
mfp (1.33 MeV)	2.49 cm	2.25 cm	1.63 cm
t (1.33 MeV)	0.13 cm	0.12 cm	0.08 cm
mfp (1.17 MeV)	2.32 cm	2.10 cm	1.47 cm
t (1.17 MeV)	0.12 cm	0.11 cm	0.08 cm

Thus a factor of 0.95 could be accounted for by an additional thickness slightly more than 1mm of Cobalt or Stainless Steel or less than 1mm of lead. For a factor of 0.9 the thicknesses can be approximately doubled.

If the hypothetical extra layer is penetrated other than normally then the required thickness is reduced by cos θ where θ is the angle to the normal. Thus a layer of lead 1.33mm thick penetrated at 30° could reduce a result by a factor 0.9.

At energies lower than the source energy the thickness required for a given attenuation is even less. This means that the observed discrepancy between the FG and Mesh models could be accounted for by small differences in the geometry.

Examining the Energy Deposition results of Figure 8 shows the ratio of mesh results over FG for energy deposition as a function of radius. The main characteristics are:

r < 7:	M/FG shows big spikes > 1.0
6 < r < 24	M/FG principally between 0.9 and 0.92.
r > 24	M/FG almost constant at about 0.93 - 0.94

A possible explanation is that there is excess material near the Z axis which absorbs extra energy and gives the observed spikes > 1.0.

In the intermediate range, the extra collisions in the Mesh cases alter the spectrum from that in the FG case. On entry into the lead (at about r = 7) the extra, degraded gammas in the Mesh cases (produced, perhaps, by Compton scatter in additional steel) are rapidly absorbed by the lead.

At depth (primarily in lead) the spectra become the same and the differences are a legacy of the earlier perturbation.

This behaviour suggests that there are model differences in the central part of the geometry where the source rods and basket are defined.

3.2.3. Examination of Mesh Model 1

The first check was to compare the material volumes for the FG case and the Mesh Model 1 case. The comparison shown in table II:

Table II Comparison of the material volumes in the FG case and Mesh model 1

Material	FG	Mesh	difference FG/M
Lead	320,450	319,995	-0.14%
Co + clad	389.48	412.84	+6.00%
Stainless	46,506	46,475	-0.067%

The lead shielding and stainless steel volumes appear to be in good agreement but the volume of the rods is significantly different in the two models. In the FG model, the outer radius of the cobalt section of a rod and its clad is 4.10mm. Its volume would be increased by 6% (to match

the Mesh model) if its radius were increased by 0.12mm. This would lead to some additional attenuation but not enough to account for the observed differences in results.

Figure 7 shows a slice through a source pin of the mesh model. The area covered by the source (shaded) has a radius 0.35cm. The outer radius of the smeared cobalt and clad should be 0.41 i.e. a thickness of 0.06 around the source. The section through the pin is extremely irregular so the expected thickness 0.06cm is not matched in any given direction. Whether it is exceeded or diminished is not obvious.

Figure 7. Section through a source rod in model 1.

To confirm that the problems originate in the inner part of the flask a hybrid input file has been created (hybrid 1) in which the detail within the basket of the FG model is replaced by a single zone that is a window on the Mesh 1. The hybrid model contains explicit FG representation of the flask structure and shield with a visible Mesh model of the interior of the basket. Figure 8 shows a section through the basket region of the hybrid model.

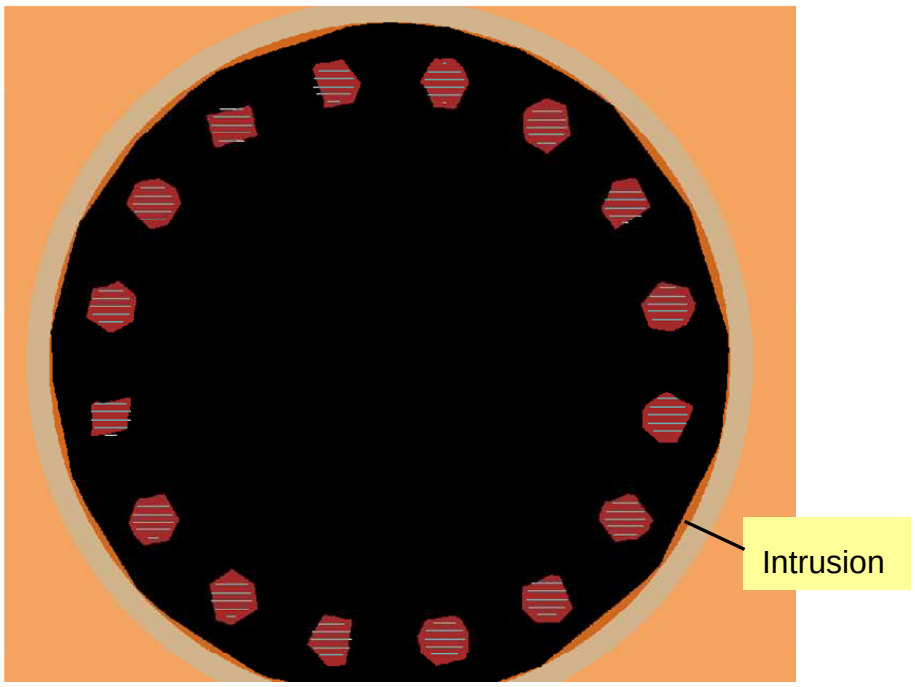

Figure 8. Section through the source basket in the hybrid model 1.

Figure 8 is quite revealing. As well as showing the irregularity of the rods it shows an intrusion of the inner liner of the shield layers from the Mesh model (dark orange) into the air space inside the FG model of this liner (black).

When a cylinder is represented as an inscribed polyhedron the volume of material within it is reduced. When such a cylinder is air then the lost air volume becomes replaced by something else: in this case steel.

The polygon section of the air space in the above figure is not regular but appears to have about 16 sides. The maximum thickness of the intruding steel will therefore be about 0.12cm. Perversely, the points of maximum thickness appear generally to be opposite a source pin - at least in this specific section.

A similar effect occurs at the interface of the steel liner and the lead shield in the full Mesh model. This is not visible in the hybrid since the interface is in the part modelled by FG. In the Mesh case, part of the steel liner will become lead (in the way that air became steel) leading to higher attenuation on entry to the lead annulus.

3.2.4. Examination of Mesh Model 2

A comparison of the material volumes is shown in Table IV:

Table IV Comparison of the material volumes in the FG case and Mesh model 2

Material	FG	TETMESH	difference FG/T
Lead	320,450	320,190	-0.08%
Co	289.56	354.35	+22.37%
Stainless Steel 'clad'	99.92	173.24	+73.37%
Stainless Steel	46,506	46,197	-0.66%

In the FG model, the outer radius of the cobalt section of a rod is 4.0mm. Its volume would be increased by 22% (to match the Mesh model) if its radius were increased by 0.42mm.

The stainless steel cladding of the rod is not a simple annulus since it has end caps and other details. If the additional volume is attributed to a simple thickening of the clad then its thickness would increase from 0.1mm to 0.17mm.

Thus the additional thickness of Co/stainless steel round the source would be of the order 0.59mm. Normal penetration through such a layer would give an attenuation of about 0.97.

As before, a hybrid geometry has been created in which the contents of the basket are represented by a Mesh hole and the rest of the model by explicit Mesh zones. A section through the basket is shown in figure 9.

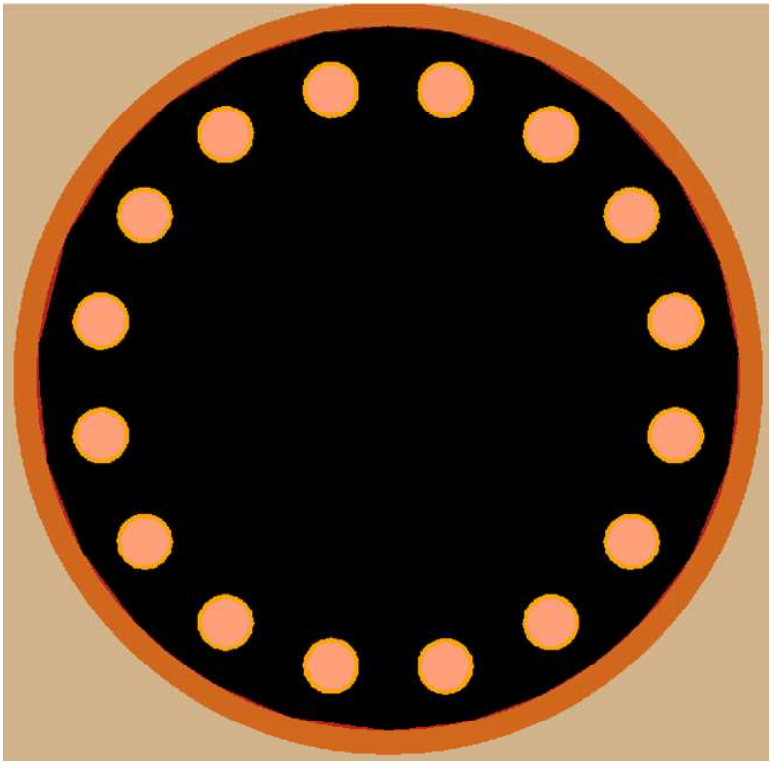

Figure 9. Section through the source basket in the hybrid model 2.

Here the cobalt rods are seen to be properly represented and the cladding is present rather than smeared with the rods. The intrusion of steel from the liner (red) caused by the polygon form of the airspace is visible but less intrusive than that in model 1.

3.2.5. Flask Model results

Figure 10 shows the ratio of the Gamma-ray dose results for the Hybrid cases with the FG case. The original mesh results are retained for comparison.

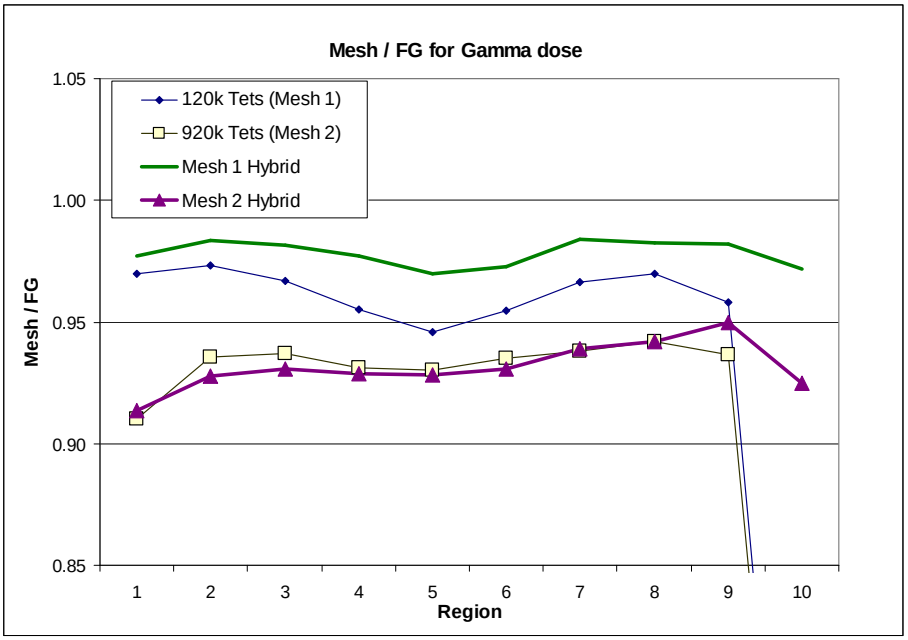

Figure 10. Ratio of FG result to the Mesh model result.

The results for region 10 no longer show the large underestimate. The hybrid model re-produces the 1mm streaming gap (mentioned earlier) exactly so this result indicates that the incomplete modelling of the streaming gap in the Mesh models was responsible for the underestimate.

Earlier it was noted that the boundary between the lead and its inner steel liner has some lead substituted for steel in the full Mesh models. At the outer lead/steel boundary the converse will apply. For results outside the flask these two effects will tend to cancel so they are not expected to significantly affect Mesh/FG ratios attributed to changes in the basket. It should be noted that the courser mesh model 1 has improved overall agreement so the cancelling effect may not have been as important for this case.

In other respects the ratio of the Mesh models to their respective FG models are consistent between the full Mesh cases and the hybrid ones. This confirms that the main differences between the Mesh and FG models are generated in the basket/rod regions.

Figure 11 shows the ratios of the energy deposition results for the Hybrid cases with the FG case. The original mesh results are retained for comparison. Unlike the gamma dose results, the energy depositions see progressively more of the shield materials with increasing radial mesh number.

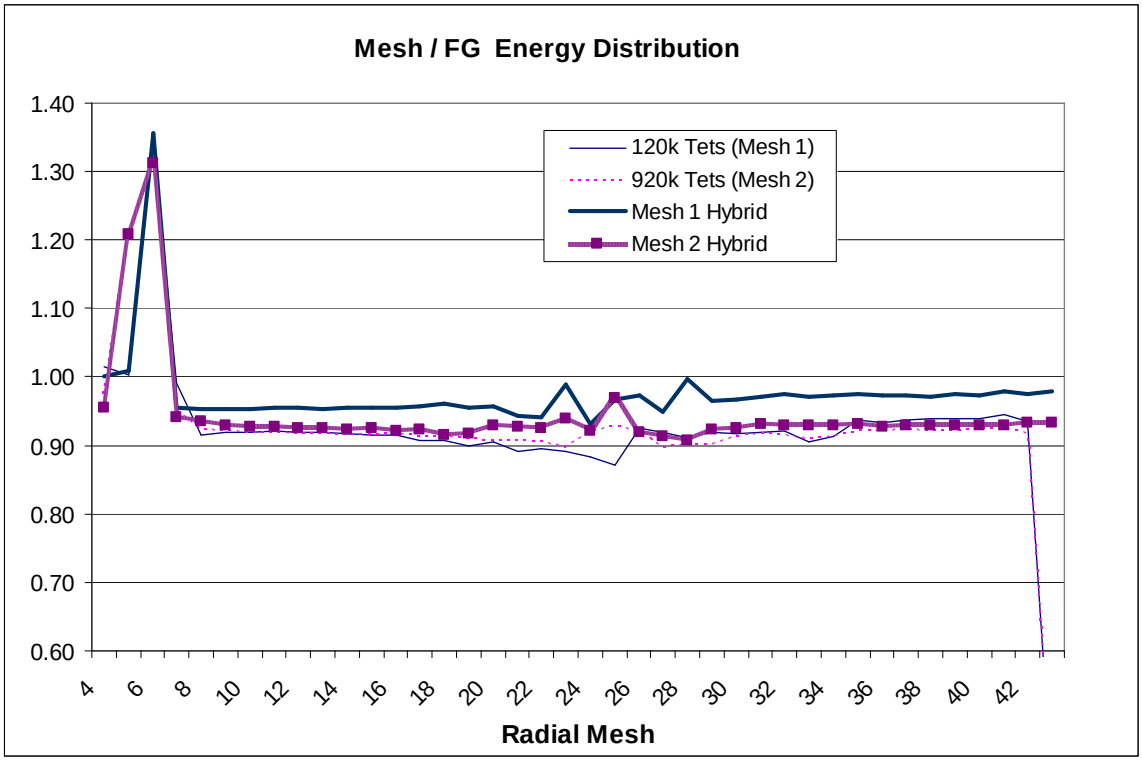

Figure 11. Ratio of FG results to the Mesh model results.

Comparison of Mesh 1 with Mesh 1 hybrid suggests that differences in the basket/rod region of the Mesh and FG models accounts for most, but not all of the differences in results. Recall that at the inner steel/lead liner there will be a substitution of some lead for steel in the full Mesh that is not visible through the window part of the hybrid model. This introduces extra attenuation into the former. Beyond this point only the residual effect of the rod/basket region remains.

There is a similar pattern in the Mesh 2 compared with Mesh 2 hybrid results but it is less pronounced because the steel/lead and lead/steel interfaces are better represented in model 2.

The result in the final radial mesh is far better for both hybrid cases indicating that the underestimate is caused by small differences in the mesh representation of the flask fins.

3.2.6. Summary of Flask Model Results

For the materials and source energies used in the problem the differences may be attributed to differences in material thicknesses of the order 1 - 2mm

Several small differences in material thicknesses have been observed in slices through the two types of model.

Additional differences have been inferred by evaluating the volumes of material in each model.

The differences in results are almost reproduced in a hybrid model in which only the rod/basket region of the flask is represented as a Mesh while the rest is modelled in FG. This suggests that the principal differences are confined to this region.

4. CONCLUSIONS

A mesh representation will never be exactly equivalent to an FG model when volumes with curved surfaces are represented by a collection of tetrahedra.

If an FG model is a correct equivalent of a Mesh representation there are no significant differences that cannot be attributed to the approximation of primitive bodies by tetrahedra.

The observed differences in the analysed models are generally less than 10% which is probably trivial compared to the safety factors that would be applied in any practical shielding calculation.

If similar differences are apparent for criticality calculations then the Mesh Hole should be used with caution.

In the flask model it is probable that the FG results are 'correct' (within the constraints of nuclear data, collision processing, scoring statistics etc.) and the Mesh results are an approximation. In a model with shapes that cannot be represented by FG bodies (for example the domed end of a pressure vessel that is not hemispherical or ellipsoidal a Mesh model might be the more accurate.

ACKNOWLEDGMENTS

MCBEND and MONK are developed under a collaboration agreement between Serco and Sellafield Ltd. The authors wish to acknowledge the members of the MCBEND & MONK development team: Ted Shuttleworth, Malcolm Armishaw, Geoff Dobson, Adam Bird, Christopher Dean, Ray Perry, (all Serco), Simon Connolly, Richard Neal, David Dewar and Keith Searson (all Sellafield Ltd).

REFERENCES

1. P. COWAN, E. SHUTTLEWORTH, A. BIRD and A. COOPER, "The Launch of MCBEND 10", *Proc. 10th International Conference on Radiation Shielding (ICRS-10) and 13th Topical Meeting on Radiation Protection and Shielding (RPS-2004),* Funchal, Madeira Island, Portugal (May 2004)
2. M. J. ARMISHAW and A. J. COOPER, "Current Status and Future Direction of the MONK Software Package", *Proc. 8th International Conference on Nuclear Criticality Safety*, St.Petersburg, Russia, May 28 - June 1 2007, (Vol II p264)
3. K. SEARSON, R. NEAL and A. J. COOPER, “Importing CAD data for Shielding and Criticality calculations with MONK and MCBEND”. *Proc. 11th International Conference on Radiation Shielding (ICRS-11) and 14th Topical Meeting on Radiation Protection and Shielding (RPS-2008),* Georgia, USA, April 13-18 2008.
4. T. BARKER, A. J. BIRD, R THETFORD, and A. J. COOPER, “Use of Tetrahedral Mesh Geometry to import a converted CAD file for Shielding and Criticality calculations with MONK and MCBEND”. *Proc. 11th International Conference on Radiation Shielding (ICRS-11) and 14th Topical Meeting on Radiation Protection and Shielding (RPS-2008),* Georgia, USA, April 13-18 2008.
5. E.J.Shuttleworth, “The Verification of Monte Carlo Codes in Middle Earth”. *Proc. 8th International Conference on Radiation Shielding (ICRS-8),* Arlington, Texas, USA, 1994.
6. D. DEWAR, A. J. COOPER, A. J. BIRD and P. COWAN, “Visual Workshop as the single model viewer for the ANSWERS Shielding and Criticality Codes”. *Proc. 11th International Conference on Radiation Shielding (ICRS-11) and 14th Topical Meeting on Radiation Protection and Shielding (RPS-2008),* Georgia, USA, April 13-18 2008.